

## Configurational Microphase Separation in Elongational Flow of an Entangled Polymer Liquid

Mohammad H. Nafar Sefiddashti, Brian J. Edwards,\* and Bamin Khomami†

*Department of Chemical and Biomolecular Engineering, Materials Research and Innovation Laboratory, University of Tennessee, Knoxville, Tennessee 37996, USA*



(Received 22 August 2018; published 14 December 2018)

Manufacturing of plastics is typically performed via flow processing of a molten polymeric fluid. Until recently, conventional knowledge has maintained that the deformation of the constituent molecules under flow is homogeneous and obeys Gaussian statistics. In this study via virtual experimentation, an entangled polyethylene melt subjected to planar elongational flow displays an unanticipated microphase separation into a heterogeneous liquid composed of regions of either highly stretched or tightly coiled macromolecules, thus providing a natural realization of a biphasic coil-stretch transition.

DOI: [10.1103/PhysRevLett.121.247802](https://doi.org/10.1103/PhysRevLett.121.247802)

The polymer and matrix composite industries represent roughly 15% of the manufacturing segment of the U.S. gross domestic product and about 3% of the total. These industries produce a huge variety of products ranging from simple household items to state-of-the-art electronic components, including many high-performance composites used in aeronautical, military, and biomedical applications. The flow of polymeric fluids is therefore of fundamental and practical interest since most polymeric materials are processed in the liquid state; however, quantifying the complicated response of polymeric fluids to hydrodynamic forces arising in manufacturing operations has posed tremendous challenges in developing models and simulations that can accurately predict the dynamical behavior of polymeric flows.

Many plastics processing operations involve elongational flow of a polymer melt in which the fluid is stretched in one direction while being simultaneously compressed in at least one orthogonal direction. Theoretical models of polymeric liquids undergoing elongational flow invariably provide similar descriptions of the microstructural response of the constituent macromolecules; i.e., with increasing flow strength quantified in terms of the dimensionless Deborah number ( $De$ ), the chains stretch out and align in the direction of flow and compress in the direction perpendicular to the flow [1–3]. The average configurational state of the fluid is assumed to possess a unimodal Gaussian distribution of chain extension, which increases in height and decreases in width as  $De$  increases, with the peak also shifting to higher values of molecular fractional extension  $x$  for higher flow strengths; see the inset in Fig. 1(a). This generic behavior is generally assumed to hold true for all types of flexible macromolecular liquids ranging from unentangled dilute solutions of polymer molecules dissolved in organic or aqueous solvents to highly entangled concentrated solutions and polymer melts.

Despite the prevailing view, in 1974 de Gennes used the elastic dumbbell model of kinetic theory [2] to demonstrate that dilute solutions of polymers undergoing planar elongational flow (PEF) could exhibit multiple steady-state configurations at  $De \approx 1$ , where the ratio of the timescale of the macromolecular stretching  $\tau_R$  (the “Rouse time”) and the timescale of the imposed flow  $\dot{\epsilon}^{-1}$  ( $\dot{\epsilon}$  being the strain rate) were approximately equivalent [4]. Two of these states were determined to be stable (i.e., a bistable equilibrium), one corresponding to a relatively coiled configuration and the other to a relatively stretched state. Consequently, the configurational microstate of the system in the vicinity of  $De \approx 1$  was apparently flow-history dependent and, thus,

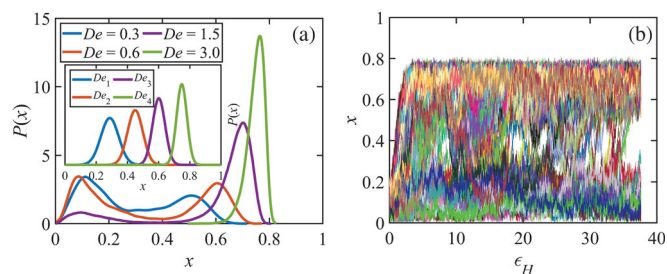


FIG. 1. Plots of the probability distribution function of the fractional molecular extension relative to a chain’s maximum possible extension,  $L_{\max}$ . (a) Inset displays idealized data at four values of Deborah number such that  $De_1 < De_2 < De_3 < De_4$ . (a) Main plot displays actual simulation data of the liquid at several values of flow strength in the proximity of  $De \approx 1$ . A bimodal distribution is evident at intermediate values of  $De$ , implying that individual molecules are occupying two independent configurational states, on average. This bimodality disappears at higher flow strengths ( $De = 3.0$ ) as the system returns to a single configurational state. Panel (b) displays the fractional extension of each molecule within the simulation box as a function of Hencky strain from the onset of flow at  $De = 1.5$ .

possibly giving rise to a hysteresis in the flow profile that de Gennes dubbed the “coil-stretch transition.” Despite the initial theoretical prediction of the coil-stretch transition, a debate ensued regarding the reality of a bistable steady-state configuration [5,6]. In view of the inherent difficulties associated with controlled elongational flow measurements, it was not possible at the time to perform experiments that could resolve the issue.

Toward the end of the 20th century, advances in experimental instrumentation had evolved to the point where direct visualization of macromolecular configurations could be implemented under a precisely controlled elongational flow. Perkins *et al.* [7] and Smith and Chu [8] were able to visualize the configurations of individual fluorescently labeled DNA molecules in dilute solution undergoing PEF and observed that otherwise identical molecules extended under flow to widely varying lengths over a broad range of timescales. Schroeder *et al.* performed similar visualization experiments on fluorescently dyed DNA molecules in dilute solution subjected to PEF over a wide range of  $De$  [9]. Two distinct experiments were conducted at each value of strain rate  $\dot{\epsilon}$  to determine if a hysteresis was evident in the macromolecular configurational response: one in which the strain rate was imposed from the equilibrium (no-flow) state and another in which  $\dot{\epsilon}$  was reduced to the equivalent value of the first experiment after prestraining the material at a relatively high rate ( $De > 5$ ). Evidence of a bistable steady state was clearly observed in the range of  $De \in [0.3, 0.6]$ , implying a hysteresis behavior in the flow profile which was very similar to that predicted by de Gennes 30 years prior.

Dilute solutions, such as those studied by de Gennes and the visualization experimentalists, are composed of independent polymer molecules dissolved in a low molecular weight solvent at a concentration low enough such that the individual macromolecules do not interact with each other; however, industrial processes of plastics and fibers are primarily involved with concentrated solutions and melts, which are typically composed of densely packed and highly entangled molecules. Theoretical and experimental studies of the coil-stretch transition to date have primarily examined dilute solutions because they are relatively easy to analyze, both theoretically and experimentally. From an experimental perspective, visualization of individual chains in a dense liquid or melt is very difficult for a variety of reasons, not the least of which is because the individual polymer chains mutually interact with each other, thereby influencing the bulk liquid’s macroscopic dynamical behavior.

Although traditional laboratory experiments of entangled polymeric liquids undergoing PEF are quite difficult to conduct, virtual experimentation can now be considered as a reliable alternative in certain circumstances. In the present case, the term “virtual experimentation” refers to atomistic computer simulations that track the phase-space trajectory of the system in response to an imposed PEF velocity

gradient by solving Hamilton’s equations of motion for the position and momentum of each atom. This is accomplished via equilibrium and nonequilibrium molecular dynamics (NEMD) simulations of realistic atomistic chains at actual experimental state points. NEMD simulations of a mono-disperse, linear  $C_{1000}H_{2002}$  polyethylene melt were performed in the NVT statistical ensemble at 450 K and the experimental density of  $0.766 \text{ g/cm}^3$  using the Siepmann-Karaboni-Smit (SKS) united-atom potential model [10]. This potential model considers each carbon atom along the polyethylene chain, together with its bonded hydrogen atoms, as a united-atom particle which interacts with its neighboring atoms, both those on the same molecule and surrounding atoms from other molecules, as sites of energetic interaction that are used to quantify the net force experienced by each atom appearing in Hamilton’s equations of motion. The SKS model has been used in many studies of alkane and polyethylene fluid behavior and is well recognized for providing a very realistic physical description of the thermodynamic and rheological properties of polyethylene liquids under both quiescent and flow conditions. The simulations involve the simultaneous solution of  $6N$  differential equations, six for each atom’s position and momentum coordinates where the number of atoms  $N$  can range up to 2 000 000. Hence, the computational methodology must be highly parallelized and implemented on massively parallelized platforms to attain steady-state conditions and provide statistically reliable data. (See Supplemental Material [11] for simulation details.)

Virtual experimentation of the sort described above recently revealed a new, unexpected phenomenon for PEF of a  $C_{1000}H_{2002}$  liquid; i.e., a bimodal distribution of molecular extension was observed at intermediate flow strengths in the range of  $De \in [0.3, 1.5]$ ; see Fig. 1(a) [32]. This observation was counterintuitive, especially in view of the almost universal prediction of rheological theory which enunciated unimodal distributions at all values of  $De$ , such as the case depicted in Fig. 1(a) (inset). These two peaks correspond to a tightly coiled configurational state and a highly stretched state at intermediate  $De$ , thus providing clear evidence of a bistable steady state, which occurs in an entangled dense liquid rather than a dilute solution. Furthermore, the two configurational states apparently coexist; it is not simply a case of one state or the other being present, as might have been intuitively expected; see Fig. 1(b). As such, virtual experimentation provided initial insight into the world of entangled polymer melts that exhibited an underlying similarity to the coil-stretch transition and hysteresis first envisioned by de Gennes for dilute solutions [see Fig. S1(a) of the Supplemental Material [11]], which could not have been achieved using traditional laboratory experimentation [32]. However, the true nature of the bistable steady state observed in the entangled polyethylene liquid had yet to be revealed.

Figure 2 displays snapshots of the  $C_{1000}H_{2002}$  melt undergoing PEF at a flow rate of  $De = 0.6$  at a randomly

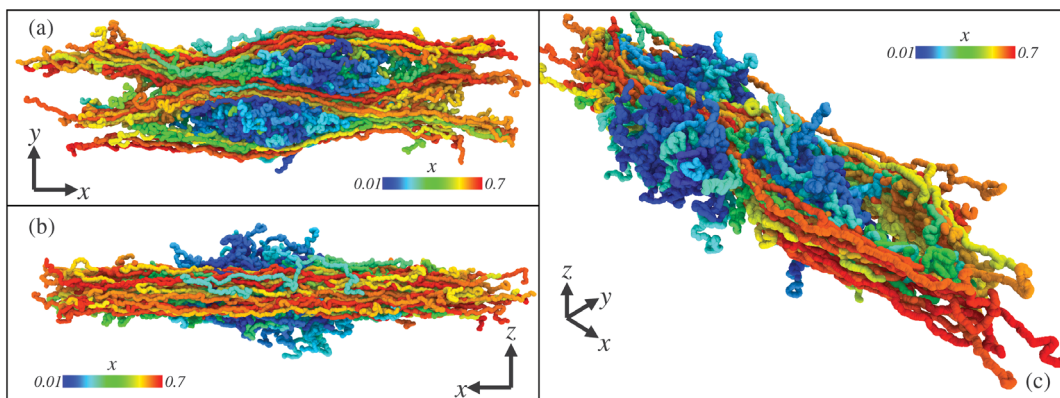


FIG. 2. Snapshots of the simulated liquid undergoing steady-state planar elongational flow ( $De = 0.6$ ) at a randomly selected time instant. Panel (a) shows the simulation cell in the extension-compression ( $x$ - $y$ ) plane as viewed along the neutral direction ( $z$ ). Cool colors (blue, aqua) represent relatively coiled molecules, whereas warm colors (orange, red) correspond to highly stretched chains; the color scale ranges over the fractional extension ( $0 \leq x \leq 1$ ) of each molecule. Panel (b) displays the same simulation cell but viewed along the axis of compression ( $y$ ). Panel (c) provides a full perspective view of the simulation cell from a nonorthogonal direction. Note that in all three panels, the highly extended chains are visualized slightly beyond the confines of the simulation cell due to the periodic boundary conditions.

chosen time instant. The Hencky strain  $\varepsilon_H = \dot{\varepsilon}t$  not only provides a quantitative measure of the dimensionless time but also of the relative deformation of the material [1]. In these snapshots, molecules with small extensions are coded with cooler colors, whereas highly extended chains are shown in warmer colors. It becomes clear from Fig. 2 that the bistable configurational states not only coexist but also that the constituent molecules become segregated via an inhomogeneous microphase separation into large domains of relatively coiled molecules that are surrounded by thinner regions of highly stretched chains. The coiled domains consist of entangled molecules, similar to the entire system at equilibrium, whereas the stretched regions are almost devoid of entanglements: The average entanglement number per chain  $Z_k$  (calculated using the Z1 code of Kröger [33]) is 25.1 at equilibrium but 21.3 within the coiled domains and 5.6 within the stretched domains at  $De = 0.6$  [see also Figs. S1(b) and S6 in the Supplemental Material [11]]. Figures 2(a) and 2(b) display the simulation cell looking down the  $z$  and  $y$  coordinate axes, respectively, revealing that the highly stretched molecules effectively form planar sheets that weave between the spheroidal domains of coiled molecules forming a heterogeneous, biphasic system. Such a startling behavior represents a remarkable departure from the theoretical expectation. To ensure that this phenomenon was not influenced by the size of the simulation cell or its periodic images, a much larger simulation cell ( $9\times$  the original) was also employed, yielding essentially the same results (see Supplemental Material [11] and Fig. S2).

The time evolution of the liquid upon application of PEF from the quiescent state at  $De = 0.6$  is shown via a series of snapshots at various time instants in Fig. 3. The biphasic microstructure develops slowly over time in a two-stage process: During the first stage, some of the molecules are

highly elongated, whereas others remain tightly coiled. In the second stage, the coiled and stretched chains form into spheroidal domains or thin sheetlike regions, respectively. Hence, the characteristic timescale of the first stage is that of macromolecular stretching, whereas that of the second stage is somehow associated with a diffusive-type process. Furthermore, the molecules within the coiled domains are highly entangled with each other [see Fig. S1(b) in the Supplemental Material [11]], which is a process governed by a timescale that is likely much longer than the timescale of stretching.

The region of flow strength where the biphasic state exists is roughly  $De \in [0.3, 1.5]$ , as evident in the snapshots displayed in Fig. 4. At  $De = 0.06$ , all molecules remain in coiled configurations, and the uniphase microstructural state is only slightly more extended than the equilibrium case. Furthermore, for  $De > 2$ , a unimodal configurational distribution is once again evident, consisting only of highly elongated molecules oriented in the flow direction. Within the biphasic flow regime, however, the size and number of the coiled domains, and concomitantly that of the surrounding sheetlike layers, are highly dependent on flow strength.

The configurational microphase separation evident in Figs. 2–4 is similar to the segregation of chemical species that occurs in microphase separation of block copolymer systems based on Flory’s thermodynamic theory of polymer solutions [34–36]; however, whereas multiphase systems of block copolymers are generated from unfavorable energetic interactions between the immiscible blocks, there is obviously no such energetic effect active in a polymer liquid composed of identical molecules. The reason that the phase separation occurs in the polyethylene melt is probably related to the effects of the imposed PEF on the free energy of the system. The Helmholtz free energy  $A$  consists of an energetic and an entropic contribution,

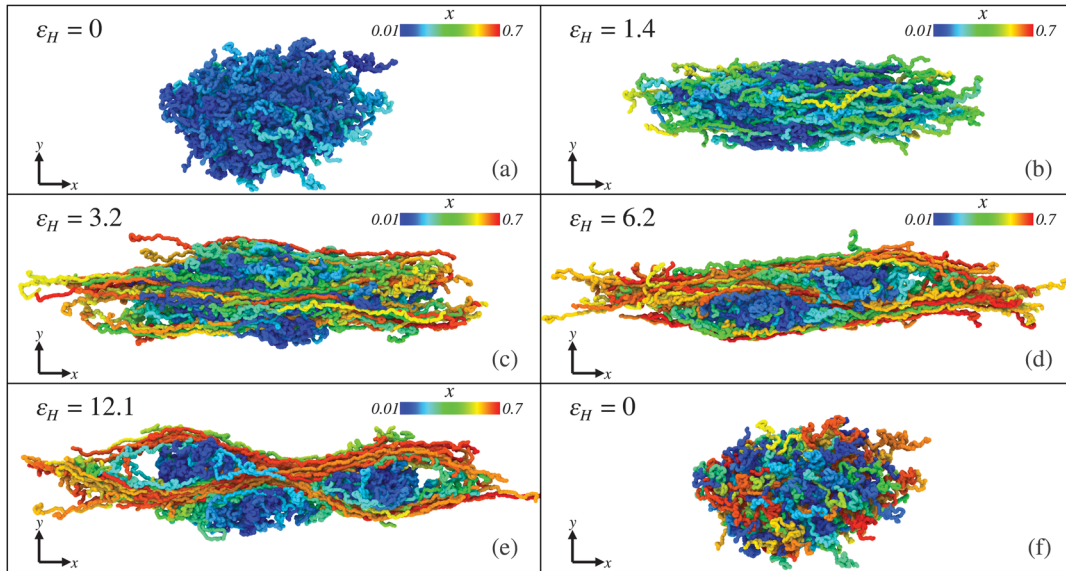


FIG. 3. Snapshots of the liquid undergoing PEF at  $De = 0.6$  as viewed from a perspective above and perpendicular to the flow-compression ( $x$ - $y$ ) plane. Panel (a) displays the equilibrated liquid under quiescent conditions. Initially, all the molecules occupy random coil configurations. Panels (b)–(e) show the development in time of the biphasic system as certain molecules greatly elongate, whereas others remain relatively coiled as dimensionless time (measured in units of Hencky strain) evolves. At long time, a steady-state condition is attained (after  $\varepsilon_H \approx 5.5$ ) in which coiled molecules have migrated into spheroidal domains, and elongated molecules have formed into thin sheetlike layers that separate the coiled regions. Panel (f) shows the same snapshot as panel (a) at  $\varepsilon_H = 0$  except that the molecules in panel (f) have been colored the same as their images in panel (e) at steady state. Note that empty spaces in some images are merely artifacts of the periodic image maps from visualizing the liquid and are not actually present within the cell.

such that a change in free energy (at constant temperature  $T$ ) is expressed as  $\Delta A = \Delta E - T\Delta S$ , where  $E$  and  $S$  are the internal energy and entropy, respectively [3]. According to the principle of virtual work, the stress exhibited by a fluid

is assumed to result from a minimization of the system free energy. Statistically, any extension of the molecules results in an entropic penalty to the free energy; hence, there is a strong statistical incentive for the chains to remain coiled.

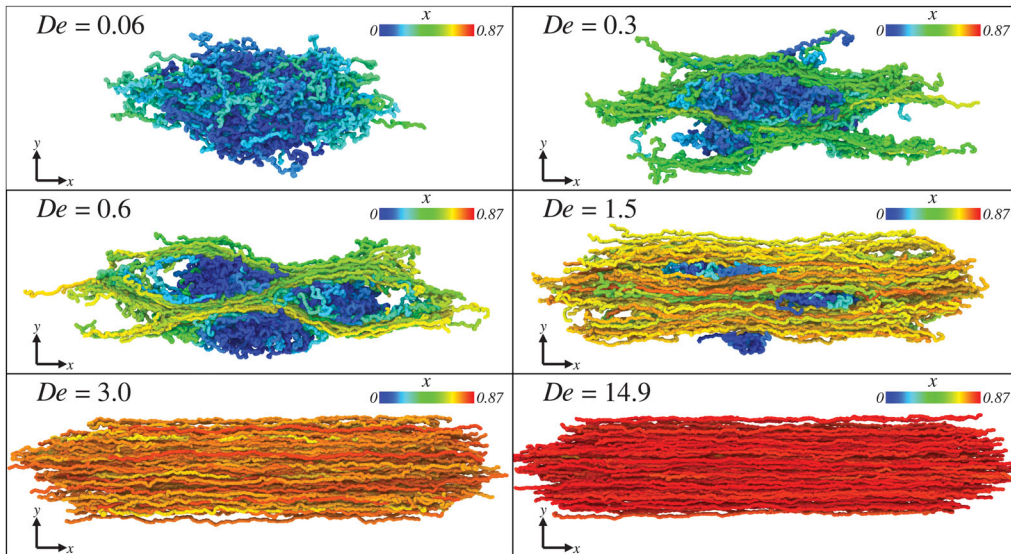


FIG. 4. Snapshots of the polyethylene liquid taken at steady state of planar elongational flow for a wide range of flow strengths. At low flow strength,  $De = 0.06$ , the overall molecular extension is relatively minor, and the chains remain coiled with the fractional extension displaying a unimodal distribution. As flow strength increases to  $De = 0.3, 0.6$ , large spheroidal domains of coiled molecules are sandwiched between thin layers of highly stretched chains. At larger flow strength ( $De = 1.5$ ), the size of the coiled domains shrinks, and the layers of extended chains grow thicker. At high flow strengths ( $De = 3.0, 14.9$ ), the coiled domains have disappeared, and only unimodal distributions of highly elongated chains are observed.

Nevertheless, the applied PEF will coerce at least some of these molecules to extend. On the other hand, Ionescu *et al.* have shown that highly elongated polyethylene chains stacked side by side exhibit very favorable energetic nonbonded intermolecular Lennard-Jones interactions, which effectively lower the system energy [37,38] similar to the nematic ordering that occurs in liquid crystals. Consequently, there is apparently a delicate balance of energetic and entropic effects at play in this system which result in the configurational microphase separation observed in Figs. 2–4 as the overall fluid system optimizes its overall energetic state in accord with the laws of physics.

It bears emphasizing here, once again, that the PEF flow cell is composed of completely identical polyethylene molecules, which effectively eliminates many arguments concerning the physical origin of this microphase separation. In what appears at first glance to be a very similar system composed of a bidisperse blend of a highly entangled host polymer containing a sizable fraction of much smaller chains, Olmsted and Milner observed a similar phase separation when the free energy bonus caused by orientation of the longer molecular component compensated for the free energy demixing cost of segregating out the shorter (and much smaller relaxation time) component [39]. Clearly, this mechanism is not valid in the present case since the molecules comprising the coiled and stretched domains are identical; hence, there must be something more subtle underpinning the configurationally induced demixing, such as a “dissipative structure” (a term coined by Prigogine but inspired by Onsager’s hypothesis of minimum dissipation) formed to reduce the system dissipation; see the Supplemental Material [11]. As observed in the visualization experiments described above [7,8], the identical DNA molecules under PEF in dilute solution took on coiled or stretched configurations almost randomly, seemingly as some undetermined function of their initial configurations. The same appears true for the entangled  $C_{1000}H_{2002}$  melt [32]; see Fig. 1(b). Once the identical molecules have attained steady-state (or at least long-lived) configurations, the chains are no longer identical, and they develop a configurational bias that drives the stretched chains to segregate to reduce the intermolecular Lennard-Jones energy, thus inducing a nematic-type ordering. Meanwhile, the coiled chains aggregate into separate domains wherein they entangle with each other and effectively dissolve within themselves to maximize their individual and collective entropy. Hence, the two classes of chain conformation, coiled and stretched, effectively develop an internal demixing free energy that drives a truly configurational microphase separation.

Although unexpected, the microphase separation observed in the simulations possibly has precedent in other flows of polymeric fluids. Recently, the phenomenon of shear banding has become accepted, in which spatially inhomogeneous regions of stress develop under seemingly

homogenous shear flows; this phenomenon has been observed in both experiment [40,41] and simulation [42–44], and the origins of this effect are currently under debate. For elongational flows, the possibility of a microphase separation might offer a plausible explanation for the common observation that the extensional viscosity of polymer solutions can thicken (grow) with increasing  $De$ , whereas polymer melts invariably display a thinning (decreasing) viscosity [45–47]; i.e., a microphase separation occurring within the dense liquid could provide a significant degree of stress relief where most of the tension was contained within the sheetlike regions of highly extended molecules. Further implications of this new phenomenon of configurational microphase separation under elongational flow are likely to puzzle polymer physicists for years to come.

Computational resources for this project were provided by the US National Science Foundation (NSF) under Grant No. CBET-0742679 to the PolyHub Engineering Virtual Organization as well as allocation of advanced computational resources by the National Institute for Computational Sciences and the ORNL Joint Institute for Computational Sciences. Financial support was provided by NSF under Grant No. CBET-1602890. This work also used the Extreme Science and Engineering Discovery Environment, which is supported by NSF (Grant No. ACI-1548562) using Bridges (Grant No. TG-CTS150054).

\*Corresponding author.  
bje@utk.edu

†Corresponding author.  
bkhomami@utk.edu

- [1] F. A. Morrison, *Understanding Rheology* (Oxford University Press, New York, 2001).
- [2] R. B. Bird, C. F. Curtiss, R. C. Armstrong, and O. Hassager, *Dynamics of Polymeric Liquids, Volume 2, Kinetic Theory*, 2nd ed. (John Wiley & Sons, New York, 1987).
- [3] A. N. Beris and B. J. Edwards, *Thermodynamics of Flowing Systems: With Internal Microstructure* (Oxford University Press, New York, 1994).
- [4] P. G. de Gennes, Coil-stretch transition of dilute flexible polymers under ultrahigh velocity gradients, *J. Chem. Phys.* **60**, 5030 (1974).
- [5] X.-J. Fan, R. B. Bird, and M. Renardy, Configuration-dependent friction coefficients and elastic dumbbell theory, *J. Non-Newtonian Fluid Mech.* **18**, 255 (1985).
- [6] J. M. Wiest, L. E. Wedgewood, and R. B. Bird, On coil-stretch transitions in dilute polymer solutions, *J. Chem. Phys.* **90**, 587 (1989).
- [7] T. T. Perkins, D. E. Smith, and S. Chu, Single polymer dynamics in an elongational flow, *Science* **276**, 2016 (1997).
- [8] D. E. Smith and S. Chu, Response of flexible polymers to a sudden elongational flow, *Science* **281**, 1335 (1998).
- [9] C. M. Schroeder, H. P. Babcock, E. S. Shaqfeh, and S. Chu, Observation of polymer conformation hysteresis in extensional flow, *Science* **301**, 1515 (2003).

- [10] J. I. Siepmann, S. Karaborni, and B. Smit, Simulating the critical properties of complex fluids, *Nature (London)* **365**, 330 (1993).
- [11] See Supplemental Material at <http://link.aps.org/supplemental/10.1103/PhysRevLett.121.247802> for details concerning the simulations, animations, and further data and analysis, which includes Refs. [12–31].
- [12] S. T. Cui, P. T. Cummings, and H. D. Cochran, Multiple time step nonequilibrium molecular dynamics simulation of the rheological properties of liquid *n*-decane, *J. Chem. Phys.* **104**, 255 (1996).
- [13] J. D. Moore, S. T. Cui, H. D. Cochran, and P. T. Cummings, A molecular dynamics study of a short-chain polyethylene melt: I. Steady-state shear, *J. Non-Newtonian Fluid Mech.* **93**, 83 (2000).
- [14] C. Baig, B. J. Edwards, D. J. Keffer, and H. D. Cochran, Rheological and structural studies of liquid decane, hexadecane, and tetracosane under planar elongational flow using nonequilibrium molecular dynamics simulations, *J. Chem. Phys.* **122**, 184906 (2005).
- [15] C. Baig, B. J. Edwards, D. J. Keffer, H. D. Cochran, and V. A. Harmandaris, Rheological and structural studies of linear polyethylene melts under planar elongational flow using nonequilibrium molecular dynamics simulations, *J. Chem. Phys.* **124**, 084902 (2006).
- [16] T. C. Ionescu, C. Baig, B. J. Edwards, D. J. Keffer, and A. Habenschuss, Structure Formation under Steady-State Isothermal Planar Elongational Flow of *n*-Eicosane: A Comparison between Simulation and Experiment, *Phys. Rev. Lett.* **96**, 037802 (2006).
- [17] D. J. Evans and G. P. Morriss, *Statistical Mechanics of Nonequilibrium Liquids* (Academic Press, New York, 1990).
- [18] S. Nosé, A molecular dynamics method for simulations in the canonical ensemble, *Mol. Phys.* **52**, 255 (1984).
- [19] W. G. Hoover, Canonical dynamics: Equilibrium phase-space distributions, *Phys. Rev. A* **31**, 1695 (1985).
- [20] A. M. Kraynik and D. A. Reinelt, Extensional motions of spatially periodic lattices, *Int. J. Multiphase Flow* **18**, 1045 (1992).
- [21] B. D. Todd and P. J. Daivis, The stability of nonequilibrium molecular dynamics simulations of elongational flows, *J. Chem. Phys.* **112**, 40 (2000).
- [22] J. G. Oldroyd, On the formulation of rheological equations of state, *Proc. R. Soc. A* **200**, 523 (1950).
- [23] B. J. Edwards and M. Dressler, A reversible problem in non-equilibrium thermodynamics: Hamiltonian evolution equations for non-equilibrium molecular dynamics simulations, *J. Non-Newtonian Fluid Mech.* **96**, 163 (2001).
- [24] C. Baig, B. J. Edwards, D. J. Keffer, and H. D. Cochran, A proper approach for nonequilibrium molecular dynamics simulations of planar elongational flow, *J. Chem. Phys.* **122**, 114103 (2005).
- [25] B. J. Edwards, C. Baig, and D. J. Keffer, An examination of the validity of non-equilibrium molecular dynamics simulation algorithms for arbitrary steady-state flows, *J. Chem. Phys.* **123**, 114106 (2005).
- [26] B. J. Edwards, C. Baig, and D. J. Keffer, A validation of the p-SLLOD equations of motion for homogeneous steady-state flows, *J. Chem. Phys.* **124**, 194104 (2006).
- [27] N. C. Karayiannis and M. Kröger, Combined molecular algorithms for the generation, equilibration and topological analysis of entangled polymers: Methodology and performance, *Int. J. Mol. Sci.* **10**, 5054 (2009).
- [28] M. H. N. Sefiddashti, B. J. Edwards, and B. Khomami, Evaluation of reptation-based modeling of entangled polymeric fluids including chain rotation via nonequilibrium molecular dynamics simulation, *Phys. Rev. Fluids* **2**, 083301 (2017).
- [29] L. Onsager, Reciprocal relations in irreversible processes. Part I, *Phys. Rev.* **37**, 405 (1931).
- [30] L. Onsager, Reciprocal relations in irreversible processes. Part II, *Phys. Rev.* **38**, 2265 (1931).
- [31] A. Stukowski, Visualization and analysis of atomistic simulation data with OVITO—The open visualization tool, *Model. Simul. Mater. Sci. Eng.* **18**, 015012 (2010).
- [32] M. H. N. Sefiddashti, B. J. Edwards, and B. Khomami, Communication: A coil-stretch transition in planar elongational flow of an entangled polymer melt, *J. Chem. Phys.* **148**, 141103 (2018).
- [33] M. Kröger, Shortest multiple disconnected path for the analysis of entanglements in two- and three-dimensional polymeric systems, *Comput. Phys. Commun.* **168**, 209 (2005).
- [34] P. J. Flory, Thermodynamics of high polymer solutions, *J. Chem. Phys.* **10**, 51 (1942).
- [35] M. W. Matsen and F. S. Bates, Block copolymer microstructures in the intermediate-segregation regime, *J. Chem. Phys.* **106**, 2436 (1997).
- [36] G. H. Fredrickson, *The Equilibrium Theory of Inhomogeneous Polymers* (Oxford University Press, New York, 2005).
- [37] T. C. Ionescu, B. J. Edwards, D. J. Keffer, and V. G. Mavrantzas, Energetic and entropic elasticity of nonisothermal flowing polymers: Experiment, theory, and simulation, *J. Rheol.* **52**, 105 (2008).
- [38] T. C. Ionescu, V. G. Mavrantzas, D. J. Keffer, and B. J. Edwards, Atomistic simulation of energetic and entropic elasticity in short-chain polyethylenes, *J. Rheol.* **52**, 567 (2008).
- [39] P. D. Olmsted and S. T. Milner, Strain-induced nematic phase separation in polymer melts and gels, *Macromolecules* **27**, 6648 (1994).
- [40] T. B. Nguyen and A. Amon, Experimental study of shear band formation: Bifurcation and localization, *Europhys. Lett.* **116**, 28007 (2016).
- [41] S.-Q. Wang, R. Ravindranath, and P. E. Boukany, Homogeneous shear, wall slip, and shear banding of entangled polymeric liquids in simple-shear rheometry: A roadmap of nonlinear rheology, *Macromolecules* **44**, 183 (2011).
- [42] M. Mohagheghi and B. Khomami, Molecular processes leading to shear banding in well entangled polymeric melts, *ACS Macro Lett.* **4**, 684 (2015).
- [43] R. L. Moorcroft and S. M. Fielding, Criteria for Shear Banding in Time-Dependent Flows of Complex Fluids, *Phys. Rev. Lett.* **110**, 086001 (2013).
- [44] M. Mohagheghi and B. Khomami, Elucidating the flow-microstructure coupling in entangled polymer melts. Part II.

- Molecular mechanism of shear banding, *J. Rheol.* **60**, 861 (2016).
- [45] Q. Huang, O. Mednova, H. K. Rasmussen, N. J. Alvarez, A. L. Skov, K. Almdal, and O. Hassager, Concentrated polymer solutions are different than melts: Role of entanglement molecular weight, *Macromolecules* **46**, 5026 (2013).
- [46] A. Bach, K. Almdal, H. K. Rasmussen, and O. Hassager, Elongational viscosity of narrow molar mass distribution polystyrene, *Macromolecules* **36**, 5174 (2003).
- [47] A. Kushwaha and E. S. G. Shaqfeh, Slip-link simulations of entangled polymers in planar elongational flow: Disentanglement modified extensional thinning, *J. Rheol.* **55**, 463 (2011).